

Conservation paleobiology on Minami-Daito Island, Okinawa, Japan: Anthropogenic extinction of cave-dwelling bats on a tropical oceanic island

Yuri Kimura ^{Corresp., 1, 2}, Dai Fukui ³, Mizuko Yoshiyuki ⁴, Kazuaki Higashi ⁵

Corresponding Author: Yuri Kimura Email address: ykimura@kahaku.go.jp

Background. With strong environmental and geographic filtration, vertebrates incapable of flying and swimming are strongly filtered out of island ecosystems. Minami-Daito Island is an oceanic island in Okinawa, Japan that harbors the Daito flying fox (Pteropus dasymallus daitoensis), a subspecies of the fruit bat and the only extant mammal endemic to the island. However, the skeleton of an extinct cavedwelling bat and fossil guano were briefly reported in a previous study.

Methods. Here, we present anthropogenic local extinction of two species of cave-dwelling bats (Miniopterus sp. & Rhinolophus sp.) from Minami-Daito Island. Because skeletal materials did not preserve sufficient bone collagen for direct radiocarbon dating, we examined guano-like deposits based on SEM observation and Fourier-transform infrared spectroscopy (FTIR) along with stable carbon and nitrogen isotope analyses for possible indirect dating. We also examined stable carbon isotopes in bone apatite to constrain the ages of the extirpated bats, using the historical knowledge that early human settlers quickly replaced the island's native C₃ forests with sugarcane (C₄ perennial grass) plantation from 1900 onward.

Results. Our cave survey documents the remains of *Miniopterus* sp. from the island for the first time. Based on the unique taphonomic conditions (unpermineralized bones, disarticulated skeletons closely scattered without sediment cover, various degrees of calcite crystal growth around bones) and a radiocarbon age of a humic sample, we suggest that the maximum age constraint of *Miniopterus* sp. and Rhinolophus sp. is 4,640 calBP. Based on a series of analyses, we conclude that the guano-like deposits are composed not of bat guano but mainly of humic substances; however, a hydroxyapatite crust associated with bat-lying stalagmites may be derived from bat feces. Stable carbon isotope analysis of bone apatite confirmed that small populations of cave-dwelling bats persisted on Minami-Daito Island after 1900.

Conclusions. The results of this study indicate that these strayed populations remained rather small and did not leave many generations. They faced a continuously high mortality risk due to severe anthropogenic stresses on the island, where most of the forests were turned into sugarcane plantations within a few decades in the early 20th century. A result of hearing surveys suggests the latest remnants most likely disappeared on the island concurrently with the introduction of chemical pesticides after World War II. Peerl reviewing PDF | (2021:07:64153:0:2:NEW 20 Sep 2021)

¹ Department of Geology and Paleontology, National Museum of Nature and Science, Tsukuba, Ibaraki, Japan

² Institut Català de Paleontologia Miguel Crusafont, ICTA-ICP, Barcelona, Spain

The University of Tokyo Hokkaido Forest, Graduate School of Agricultural and Life Sciences, The University of Tokyo, Furano, Hokkaido, Japan

⁴ Department of Agriculture, Tokyo University of Agriculture, Atsugi, Kanagawa, Japan

Office Key Point, Minami-Daito, Okinawa, Japan





1	
2	
3	Conservation paleobiology on Minami-Daito Island, Okinawa, Japan: Anthropogenic extinction
4	of cave-dwelling bats on a tropical oceanic island
5	
6	
7	
8	
9	Yuri Kimura ^{1,2*} , Dai Fukui ³ , Mizuko Yoshiyuki ⁴ , Kazuaki Higashi
10	
11	
12 13 14	Yuri Kimura https://orcid.org/0000-0002-7621-9901 Dai Fukui https://orcid.org/0000-0002-5449-4283
15	
16	¹ Department of Geology and Paleontology, National Museum of Nature and Science, 4-1-1
17	Amakubo, Tsukuba, Ibaraki, 305-0005, Japan; e-mail: ykimura.research@gmail.com.
18	
19	
20	² Institut Català de Paleontologia Miquel Crusafont, ICTA-ICP. Edifici Z. Carrer de les
21	Columnes, s/n., Campus de la Universitat Autònoma de Barcelona. E-08193 Cerdanyola del
22	Vallès, Barcelona, Spain
23	
24	³ The University of Tokyo Hokkaido Forest, Graduate School of Agricultural and Life Sciences,
25	The University of Tokyo, 9-61, Yamabe-Higashimachi, Furano, Hokkaido 079-1563, Japan
26	
27	⁴ Department of Agriculture, Tokyo University of Agriculture, 1737 Funako, Atsugi, Kanagawa
28	243-0034, Japan
29	
30	5 Office Key Point, Minami-Daito Island, Okinawa
31	
32	

PeerJ

33	
34	
35	Keywords
86	Anthropogenic extinction; extirpation; Chiroptera; Mammalia; Conservation paleobiology;
37	Zoology; stable carbon isotopes; FTIR; fossil guano
88	
89 10	
11	Abstract
12	
13	Background. With strong environmental and geographic filtration, vertebrates incapable of
14	flying and swimming are strongly filtered out of island ecosystems. Minami-Daito Island is an
15	oceanic island in Okinawa, Japan that harbors the Daito flying fox (Pteropus dasymallus
16	daitoensis), a subspecies of the fruit bat and the only extant mammal endemic to the island.
17	However, the skeleton of an extinct cave-dwelling bat and fossil guano were briefly reported in a
18	previous study.
19	Methods . Here, we present anthropogenic local extinction of two species of cave-dwelling bats
50	(Miniopterus sp. & Rhinolophus sp.) from Minami-Daito Island. Because skeletal materials did
51	not preserve sufficient bone collagen for direct radiocarbon dating, we examined guano-like
52	deposits based on SEM observation and Fourier-transform infrared spectroscopy (FTIR) along
53	with stable carbon and nitrogen isotope analyses for possible indirect dating. We also examined
54	stable carbon isotopes in bone apatite to constrain the ages of the extirpated bats, using the
55	historical knowledge that early human settlers quickly replaced the island's native C ₃ forests
56	with sugarcane (C ₄ perennial grass) plantation from 1900 onward.
57	Results . Our cave survey documents the remains of <i>Miniopterus</i> sp. from the island for the first
8	time. Based on the unique taphonomic conditions (unpermineralized bones, disarticulated



skeletons closely scattered without sediment cover, various degrees of calcite crystal growth around bones) and a radiocarbon age of a humic sample, we suggest that the maximum age constraint of *Miniopterus* sp. and *Rhinolophus* sp. is 4,640 calBP. Based on a series of analyses, we conclude that the guano-like deposits are composed not of bat guano but mainly of humic substances; however, a hydroxyapatite crust associated with bat-lying stalagmites may be derived from bat feces. Stable carbon isotope analysis of bone apatite confirmed that small populations of cave-dwelling bats persisted on Minami-Daito Island after 1900.

Conclusions. The results of this study indicate that these strayed populations remained rather small and did not leave many generations. They faced a continuously high mortality risk due to severe anthropogenic stresses on the island, where most of the forests were turned into sugarcane plantations within a few decades in the early 20th century. A result of hearing surveys suggests the latest remnants most likely disappeared on the island concurrently with the introduction of chemical pesticides after World War II.

Introduction

Insular systems such as remote islands, volcanic lakes, and deep caves, have offered natural test grounds for understanding how migration, speciation, and extinction function in the long-term ecological dynamics of life (van der Geer et al., 2010). In these systems, geographic barriers and environmental filters yield species-poor communities with a high percentage of endemic taxa, which in most cases are endangered and have thus gained recent attention



82	regarding conservation against anthropogenic extinction. Vertebrate animals incapable of flying,
83	swimming, or more passively rafting in water are generally filtered out of the island ecosystems.
84	The oceanic Daito Islands in Japan are an archipelago of remote island that are
85	surrounded by vast oceanic water and have been separated from the closest landmass since their
86	emergence. Historically, these islands were uninhabited by humans until the first exploitation
87	over 120 years ago in 1899-1900. Prior to the arrival of humans, dense native forests comprising
88	subtropical fan palm trees (Livistona chinensis var. amanoi), Neolitsea sericea var. argentea,
89	banyans, and the evergreen shrub (Excoecaria formosana var. daitoinsularis) harbored endemic
90	species of birds, insects, and fruit bats. By the 1930s, the rapid development of cultivation and
91	sugarcane plantation along with the filling of underground caves and sinkholes for land
92	improvement and military construction caused severe and irreversible changes in vegetation
93	(Editorial Committee of the History of Minami-Daito Village, 1990). At present, any remaining
94	natural forests are limited to the rims of the islands (Fig. 1A; Google Earth, 2021).
95	Under a combination of high anthropogenic stresses and biogeographical constraints, the
96	Daito flying fox (Pteropus dasymallus daitoensis), a subspecies of the Ryukyu flying fox
97	(Pteropus dasymallus), is the only extant mammal species endemic to the Daito Islands. The
98	distribution of the Ryukyu flying fox is limited to the southwestern island chain of Japan and
99	Taiwan and small islands north of Luzon in the Philippines (Chen et al., 2021), and the Daito
100	flying fox is an endemic subspecies only inhabiting the Daito Islands, differing from the
101	neighboring subspecies Orii's flying fox (Pteropus dasymallus inopinatus) on Okinawa Island
102	and its adjacent islands.
103	Although the endangered Daito flying fox is the only native mammal on the Daito Islands
104	today, Shimojana (1978) reported a few skeletons of a cave-dwelling bat species found in





Hoshino Cave, the only tourist cave on Minami-Daito Island, and classified those skeletons as
individuals of <i>Rhinolophus</i> sp. Shimojana (1978) also noted that large amounts of fossil bat
guano were present in the cave. Cave-dwelling bats, including fossils and extant ones, have not
been documented on the island since then. Recently, based on information about additional
skeletons of insectivorous bats in a different cave on the same island, we collected skeletal
remains that belong to two species of different sizes. In this study, we aim to determine whether
guano-like deposits in the caves where skeletal remains are found are actually bat guano using a
multiproxy geochemical approach and discuss that the local extinction of the cave-dwelling bats
was probably caused by high anthropogenic stresses on the small island.



Geological Setting

119

120

121

122

123

124

125

126

127

128

129

130

131

132

133

134

135

136

137

138

139

140

141

118

The Daito Islands are an archipelago located on the Philippine Sea Plate, nearly 400 km southeast of Okinawa Island in Okinawa Prefecture, Japan, comprising Minami-Daito Island (Minamidaitōjima, 30.74 km²), Kita-Daito Island (Kitadaitōjima, 12.71 km²), and Oki-Daito Island (Okidaitōjima, 1.19km²), listed in order of decreasing surface area (Fig. 1A-B; Editorial Committee of the History of Minami-Daito Village, 1990). Oki-Daito Island is uninhabitable because of decades of firing exercises by the United States Navy, so ecological studies have only been conducted on Minami-Daito Island and Kita-Daito Island. The Daito Islands are atolls that drifted to its current position from near the equator where coral reefs began to accumulate over 50 million years ago (Klein and Kobayashi, 1980; Seno and Maruyama, 1984) and were uplifted during the Pliocene and Pleistocene epochs on the forebulge of the Philippine Sea Plate prior to subduction along the Ryukyu Trench (Ohde and Elderfield, 1992). Based on samples from boring surveys on Kita-Daito Island between 1934 to 1936, the carbonate deposits on the islands are up to 430m thick, and the oldest strata are early Miocene in age (Ohde and Elderfield, 1992). On Minami-Daito Island, Urushibara-Yoshino (2012) recognized two informal lithostratigraphic units of dolomitized limestone on the island, including the "Lower Daito Layer" and the more fossiliferous "Upper Daito Layer," which are separated by an unconformity that was interpreted as the surface of karstification. Differential erosional rates of the dolomitized limestone layers have formed the unique topography of Minami-Daito Island that is characterized by basin-shaped lowlands ("Hagu Shita" in local vernacular) of the heavily karstified Lower Daito Later surrounded by topographic highlands ("Hagu Ue" in local vernacular) of the Upper Daito Layer averaging 40m above sea level that form rims along the coast (Urushibara-Yoshino, 2012; Nambu, 2003). A coastal bench ~10m above sea level is





142	overlain by a thin coral limestone dated to ~125 ka, corresponding to the Marine Isotope Stage
143	5e during the last interglacial period in the Pleistocene (Ota et al., 1991), whereas the lowest
144	coastal bench at ~3m above sea level may have formed more recently during a mid-Holocene
145	sea-level highstand, the age of which is 6,500-5,000 BP (Umitsu, 1991 for ages; Urushibara-
146	Yoshino, 2012).
147	
148	



Materials and Methods

Skeletal remains in the caves of Minami-Daito Island

There are countless numbers of sinkholes (dolines) and caves on Minami-Daito Island, some of which preserve the remains of locally extinct bats. We collected vertebrate skeletal remains and bat guano-like deposits from two of these caves, which are a public cave called Hoshino Cave (also called *Hoshinodō* or Hoshinodo Cave, as "dō" means "cave" in Japanese) and a privately-owned cave informally called "Cave A" (Fig. 1A). Fieldwork was conducted in January 2016 and January 2018 because the CO₂ concentration levels in the caves are lowest during the winter. All fieldwork was conducted outside national parks or restricted areas designated by the Nature Conservation Act.

Cave A is accessible via several spots where the ceiling has collapsed, but we entered through the main natural entrance, which is located in the Hagu Shita basin near the basin-side edge of the Hagu Ue rim (Fig. 1C). Because there is no published map for Cave A, we made a simple route map from the main entrance to our sample locations (Fig. 1D). Skeletal remains of insectivorous bats were collected from a small hall about 60 m north of the main entrance.

Generally, skeletal remains are scattered as if these individuals have not been transported by vater flow (Fig. 2A–B). In Cave A, we observed that at least four individuals were almost completely articulated and embedded by thin crusts of flowstone, which have served as protection against dissociation and bone decay (Fig. 3). Two of these individuals were collected (Fig. 2D). For others, bones are disarticulated and selectively preserved with a bias toward long bones (radius, metacarpal, etc.), tympanic bullae, and jaws. In Hoshino Cave, we entered from a





174	natural entrance, which is not open to the public, and found an incomplete set of one individual
175	of Rhinolophus sp. several meters below a paved commercial route (Fig. 1E).
176	Fragile bones were reinforced in the lab by coating with a solution of 5% Paraloid B-72
177	dissolved in acetone. They are stored at the National Museum of Nature and Science, Tokyo
178	(NMNS; Tsukuba, Ibaraki, Japan). A complete list of collected bones is provided in Table 1, and
179	a detailed taxonomic study of the specimens is in progress.
180	Some well-preserved fragments without secondary calcite crystal growth or acid etching
181	were consumptively sampled for radiocarbon dating; however, none preserved collagen (i.e., no
182	signal was detected for nitrogen using Elemental Analysis [EA] on a bone fragment), so these
183	materials were not useful for direct dating. Because we were unable to determine the age of any
184	individual fossil, we instead examined guano-like deposits accumulated in the same caves for
185	time-averaged ¹⁴ C ages.
186	
187	
188	
189	
190	
191	
192	



194

195

196

197

198

199

200

201

202

203

204

205

206

207

208

209

210

211

212

213

214

215

Guano-like deposits on Minami-Daito Island

Guano-like deposits were sampled at four localities in Cave A (Fig. 1D) and one locality in Hoshino Cave (Fig. 1E). These deposits are accumulated on the floors of the caves and further washed downstream if large amounts are present. They are soft muddy sediments brownishblack (10YR2/2 to 10YR2/3) to black (10YR2/1) in color. Mud particles are loosely coalesced to form sand-sized granules, which are often contaminated with dolomite fragments. They are also present in local small depressions above the floor. Flowstones in the caves are often colored black from pollution in areas where the Japanese military used them as headquarters during World War II (WWII; "Headquarter Hall" on the map) and where groundwater drains. We collected guano-like deposits from large piles (Fig. 4A) or handpicked coalesced particles using forceps (Fig. 5A). The largest pile of guano-like deposits (8~10m wide on the surface) was found in Hoshino Cave, which is probably the deposit noted by Shimojana (1978). The thickness of the pile is over 50 cm at a random spot where we collected samples from its bottom, a mid-part, and its top. There is no sedimentological difference observed except that the bottom sample contained more carbonate lithic fragments. In Cave A, a thin crust under a bat-lying flowstone was also sampled (Figs. 5B, 5D). The sampled deposits were dried in a convection oven at 38°C and were sieved at 850 µm, 425 µm, and 250 µm. Samples between 250 µm and 425 µm were carefully handpicked using forceps for black particles to avoid carbonate contamination prior to further analyses. Because insectivorous bats consume arthropods (crickets, beetles, moths, etc.), bat guano contains their chitinous exoskeletons, which are resistant to decay. We utilized established signals of the chitinous exoskeletons of arthropods to determine whether or not the guano-like

deposits are guano-derived by comparison with modern and fossil bat guanos as positive



references and red soil as a negative reference.	The red soil was	collected from	the bottom of
thick soil deposits beneath a fissure in Cave A.			

Modern and subfossil bat guano as positive references

For comparison with the guano-like deposits sampled in Hoshino Cave, we used a commercial guano fertilizer collected in Indonesia (called R1 in figures; ARK Co. Ltd., Ushiku, Ibaraki, Japan), modern bat guano of *Miniopterus fuliginosus* (R2) from an unnamed artificial cave of soft sandstone in Taito, Isumi, Chiba, subfossil guano deposit (R3) from Fujido Cave in Udeno, Gunma, and fecal pellets (R4) of *Vespertilio sinensis* in Chichibu, Saitama. Localities were selected by Y.K. for ease of access. These samples were used as "positive references" for comparison with our unknown guano-like samples from the Minami-Daito Island caves (see Supplementary Article S1 for more details).

Scanning Election Microscopy (SEM) observation

In the fecal pellets of modern insectivorous bats, arthropod exoskeleton fragments are usually observed. Thus, we imaged dry samples of the guano-like deposits from Hoshino Cave and the four guano references at the National Museum of Nature and Science (NMNS; Tsukuba, Ibaraki, Japan) using a JSM-6510 (JEOL Ltd., Tokyo, Japan) scanning electron microscope (SEM) under 70x to 300x magnification. Images were taken at an acceleration voltage of 3 kV with gold sputter coating on the dry samples.

Fourier Transform Infrared Spectroscopy (FTIR)



Fourier transform infrared (FTIR) spectroscopy is a technique commonly used to characterize specific molecular structures in organic compounds. The FTIR spectra of chitin extracted from modern and fossil guano as well as those of bulk guano are well known based on previous studies (e.g., Wurster et al., 2010; Kaya et al., 2014), so we used FTIR to identify whether chitin is a major component of the guano-like deposits. The hand-picked samples of the guano-like deposits and reference materials (modern and fossil guano, red soil) were refluxed with 1.0M HCl at 80°C for at least 8 hours to remove exogenous carbonates and organic acids (e.g., fluvic acids) and were rinsed with deionized water until the solvent became a neutral pH. After drying in a convection oven below 38°C, the samples were ground in an agate mortar with a pestle. They were then stored in a desiccator at room temperature until analysis.

Each powdered sample was diluted with ground KBr, pressed into a pellet in a stainless-steel disk, and analyzed without a vacuum using a JASCO FT/IR-6800 (JASCO Inc., Tokyo, Japan) at NMNS. Pure KBr was measured as the background under the same conditions as the samples. The infrared spectra of absorbance were measured from 400 cm⁻¹ to 4000 cm⁻¹ by 64 scans at a resolution of 4 cm⁻¹ and are expressed as the percentage of transmittance (%T). Automatic baseline corrections were made using a second-degree polynomial fitting (x²).

Stable isotope analyses and C:N ratio of the guano-like samples

To supplement FTIR results of the guano-like samples, we measured stable carbon and nitrogen isotope values and mass ratios of organic carbon to nitrogen (C:N) for the HCl-treated samples using a FLASH 2000 CHNS/O elemental analyzer coupled with a Finnegan MAT253 isotope ratio mass spectrometer (Thermo Fisher Scientific, Massachusetts, USA) at NMNS. Isotopic ratios are expressed in delta notation (δ^{13} C, δ^{15} N) in parts per thousand (‰) and reported on the VPDB scale for δ^{13} C values and the AIR scale for δ^{15} N values. For guano-like deposits, a



thick sample from Hoshino Cave and a handpicked pellet-like sample from Cave A were selected for analysis. Three internal lab standards were analyzed for each run and used for data correction. Repeated analyses of the standards were within $\pm 0.2\%$ for δ^{13} C and $\pm 0.25\%$ for δ^{15} N. Carbon isotope values of guano references are used to reconstruct isotopic signals of their diet by taking the following isotope fractionation factors into consideration. The fractionation factor between the feces of insectivorous bats and their diet (i.e., insects) is known to be negligible (Salvarina et al., 2013), whereas larger fractionation factors are observed between the cuticles of insects and their diet of plant matter. In an experimental study, Gratton and Forbes (2006) showed that tissues of predacious beetles are more enriched by 2.2% relative to their aphid diet.

Stable carbon isotopes of bone apatite

Stable carbon isotope analysis of animal tissues is a useful technique to detect an isotopic signal of C_4 plants in their habitat. Although no C_4 plant is native to the Daito Islands, historical records (Editorial Committee of the History of Minami-Daito Village, 1990) document that the C_4 perennial grass sugarcane was introduced on Minami-Daito Island in 1899–1900 and increasingly replaced native C_3 forests on the island by the 1930s (see Introduction). We therefore hypothesize that any organic materials on the island with the isotopic signature of C_4 plants must have originated after the introduction of sugarcane in 1899–1900. Thus, stable carbon isotope analysis with correct applications of fractionation factors can serve as a time constraint for direct human influences on Minami-Daito Island.

Relatively well-preserved bones (no acid etching, no or limited calcite crystallization) from Cave A were selected for carbon isotope analysis of bone apatite. For each bone, the surface was



shaved off to remove calcite crystals. The powdered samples were soaked in 2% NaOCl overnight for at least 12 hours at the room temperature. After rinsing with deionized water, they were treated with buffered 0.1M acetic acid (pH=4.2) for 2 hours at 40°C until no obvious bubbles were observed, and they were neutralized with ultrapure water and dried in an oven at 40°C. The treated samples were sent to Shoko Science Co., Ltd. (Saitama, Japan) and analyzed for stable carbon isotope via a H₃PO₄ digestion using by a continuous flow Thermo Scientific Delta V Plus isotope ratio mass spectrometer coupled to a Thermo Scientific GasBench II. Of the eight samples analyzed in this study, seven come from individual bones, whereas one sample is composed of multiple small bone fragments.

The carbon isotope values of bone apatite were used to reconstruct isotopic signals of vegetation by applying experimentally known enrichment factors (ϵ^*) and an end-member mixing model. The enrichment factor applied in this study is +11.0±0.1‰ between bone apatite and insectivorous diet (Podlesak et al., 2008). For isotopic spacing (Δ) between insectivorous diets of bats and surrounding vegetation, we applied +2.2‰ or +3.0‰ based on an a dietary-switch experimental study by Gratton and Forbes (2006). For the mixing model, δ^{13} C value of -12.5‰ was used for pure C₄ vegetation in the modern time (Cerling et al., 1997), and that of -29.1‰ was applied for pure C₃ vegetation of the present. The latter was calculated based on the equation of Kohn (2010), which takes mean annual precipitation (MAP), altitude, and latitude into account. MAP of Minami-Daito Island is 1680 mm/year between 1942 and 2020, which was applied to the equation. See Supplementary Article S1 for more details.

Radiocarbon dating of subfossil guano references

We determined the ¹⁴C age of both the fossil guano reference (R3) and the guano-like samples for comparison. The same samples analyzed for stable isotopes were chosen for



PeerJ

3

310	radiocarbon dating. Prepared samples were sent to the accelerator mass spectrometry (AMS)
311	facility at the University Museum, the University of Tokyo, where the samples were further
312	prepared and measured by Compact AMS System (National Electrostatics Corp., Wisconsin,
313	USA), following their in-house protocols (Omori et al., 2017). For each sample, $\delta^{13}C$ measured
314	by AMS was used to correct for the conventional radiocarbon age (Stuiver and Polach, 1977).
315	These radiocarbon ages were calibrated by IntCal20 curves (Reimer et al, 2020) in OxCAL4.2
316	(Bronk Ramsey, 2009) and are expressed as calBP (Before Present; 0 calBP = AD 1950).
317	Preparation and analytical methods are described in Supplementary Article S1.
318	
319	
320	
321	



RESULTS AND DISCUSSION

Skeletal remains of locally extinct cave-dwelling bats

In a survey during the 1970s, Shimojana (1978) reported a few skeletons of *Rhinolophus* sp. from Hoshino Cave. In this study, we found the skeletons of single individuals of *Rhinolophus* sp. in both Hoshino Cave and Cave A. Additionally, we collected skeletons of *Miniopterus* sp. from Cave A, which represent at least 13 individuals (taxonomic study in progress). Some skeletons are articulated, but many are disconnected with associated bones closely scattered on the surface of the cave floor (Fig. 2), so we infer that they were not transported by the water after death. No traces of soft tissues such as pelage are preserved. In Cave A, we observed at least four individuals of *Miniopterus* sp. that were embedded within a thin crust of flowstone (Fig. 3), two of which were collected. No fossil remains are permineralized, but many are encrusted with calcite. The condition of calcite crystal growth on and in bones depends on the availability of mineral-rich water flow near the bones. In many bone materials, the surface is partially covered with small calcite crystals, and/or the medullary cavity of long bones is partially infilled.

Due to the lack of bone collagen for radiocarbon dating in the specimens we sampled, it is unknown whether these bat species utilized the cave contemporarily; however, because there is no difference in bone preservation and secondary crystal growth of calcite between the two species, our paleontological interpretation is that the ages of their existences do not differ even if they may not be coeval *sensu stricto*.

SEM observation of guano-like samples



Fragments of insect exoskeletons are clearly visible in both modern (Figs. 4D-4E) and fossil guano references (Fig. 4G) at or above 70x magnification although the fossil guano is degraded to be humus-like and contaminated with sediments (Fig. 4F). On the other hand, the guano-like samples appear to be aggregates of clay-sized particles with no clear presence of insect remains (Figs. 4B-4C), suggesting that they may not be composed of bat guano.

Nevertheless, because the preservation potential of chitinous insect remains is expected to be lower in guano deposits from tropical wet caves like those on Minami-Daito Island than in the fossil guano reference collected from a more temperate region, we proceeded with further analyses.

FTIR

None of the guano-like deposits collected in this study present spectral patterns characteristic of fresh or fossil guano (Figs 6, 7, see Supplementary Article S1 for full description of references). In the range between 1000 cm⁻¹ and 1800 cm⁻¹, different spectral patterns are observed between guano references and sampled deposits. Particularly, a shoulder peak at 1712 cm⁻¹ associated with C=O stretching of carboxylic acid (Dick et al., 2003) is present in guano-like samples but does not occur in the spectra of guano references (Fig. 6). This peak occurs in humified organic matter (Dick et al. 2003; Palumbo et al., 2018).

The FTIR spectrum of the guano-like sample Y180119g3 (Fig. 6D) is comparable to that of humic acid (Figs. 6H-6I). The absorption at 1078 cm⁻¹ is ascribed to the stretching vibration of oxygen bonds in aliphatic ether (Zhang et al., 2015). The presence of aliphatic compounds is consistent with the interpretation that this sample is a fraction of humic substances (Méndez, 1967). The peak at 1244 cm⁻¹ ean be interpreted as antisymmetric C-O stretching and OH



deformation in a carboxyl group, and -C-OH bending of phenols and tertiary alcohol in humic substances (Dick et al., 2003). As organic functional groups, carboxylic acids are contained in humic substances. We interpret that the guano-like deposits sampled in this study are forms of humic substances rather than fossil bat guano, with the exception of Y160114g1, which was identified as hydroxyapatite (Fig. 7D) by comparing characteristic spectral peaks with those of pure hydroxyapatite in Jayaweera et al. (2018).

The hydroxyapatite sample, Y160114g1, occurs as a thin crust light brown in color only partially exposed under a fracture of more recent flowstone on the slope of a large stalagmite (Fig. 5B). Interestingly, we found skeletal remains of at least two individual bats lying on a slope of the stalagmite, both of which are also covered by recent flowstone (Fig. 3B). The hydroxyapatite crust stratigraphically underlies the bat skeleton. As a calcium phosphate mineral, hydroxyapatite is commonly precipitated in caves where phosphorous-rich organic deposits such as bat guano or bones are supplied and interaction between the guano-derived leachate and calcium-rich water from carbonate host-rock can occur at a pH greater than 6 (Fiore and Laviano, 1991; Hill and Forti 1997; Tămaş et al. 2014; Giurgiu and Tămaş, 2013). Because this hydroxyapatite crust was found in association with a bat skeleton, and hydroxyapatite precipitation is inhibited in the presence of humic and fluvic acids (Inskeep and Silvertooth, 1998), this crust was likely derived from bat guano rather than humified plant material.

C:N ratios, δ^{13} C, and δ^{15} N values of the guano-like samples

The C:N ratios, total nitrogen by weight percent (%N), δ^{13} C values, and δ^{15} N values of the guano-like samples are shown in Fig. 8 (Tables 2, S1). In the bulk sample of the fissure-filled deposit, total nitrogen is nearly 0.1%, which is within the standard range of nitrogen content for



395	sediments (Forbes and Bestland, 2006). The nitrogen content in the fecal pellet-like sample
396	Y180119g2 (Fig. 5A) from Cave A is lower than the %N range of guano references (Fig. 8A).
397	Because the FTIR spectrum of the pellet-like sample similarly traces that of the fissure-filled
398	deposit, we interpret that the fecal pellet-like sample is a mix of sediment and organic matter. In
399	general, C:N ratios of all analyzed samples are tightly clustered, ranging from 4.2 for fissure-
400	filled deposit to 6.5 for the fossil guano reference with the unknown guano-like samples placed
401	in-between (Fig. 8B). These values are much lower than fresh plants and coals (e.g., Schmidt and
402	Gleixner, 2005) and superficially meet one of Forbes and Bestland's (2006) criteria to identify
403	fossil guano (C:N <10). Nevertheless, in our case, the low C:N values of the samples are still
404	consistent with the FTIR-based classification of the red soil of the Minami-Daito Islands as a
405	lateritic soil because it is known that C:N ratios in humic substances and soil organic matter
406	extracted from modern lateritic soil show roughly comparable values between 7 and 10 (Dick et
407	al., 2003).
408	The δ^{13} C values of guano references range from -28.2% to -19.1%, encasing the guano-
409	like samples (Fig. 8B). Accounting for the isotopic spacing among bat guano, their insectivorous
410	diet, and surrounding vegetation, the guano-like deposits are well within the range of C ₃ plants,
411	which exhibit a general range from -23‰ to -37‰ in non-desert areas (Kohn, 2010). Because
412	they completely lack a signal of C ₄ plants, it is suggested that these deposits were formed well
413	
	before anthropogenic influences because sugar cane, C ₄ perennial grass, became exclusively
414	before anthropogenic influences because sugar cane, C ₄ perennial grass, became exclusively dominant by the 1930s due to heavy cultivation on the island.
414 415	
	dominant by the 1930s due to heavy cultivation on the island.



418	$\delta^{15}N$ values above 12‰ in association with low C:N ratios below 10 and high contents of
419	$SO_3+P_2O_5+CaO$ to identify a potential guano layer in accumulated cave deposits. The $\delta^{15}N$
420	values of the guano-like samples from Hoshino Cave do not meet their criteria although neither
421	do those of some guano references.
422	Overall, as in the case of %N and C:N ratios, stable carbon and nitrogen isotopes were
423	not good indices to identify bat guano in caves of tropical islands where lateritic soil can be
424	developed.
425 426 427	Stable carbon isotopes of bone apatite
428 429	Bone apatite δ^{13} C values (n=8) show a wide range from -15.0% to -8.36% with a mean of -
430	11.5±2.38‰ (±1SD) (Table 3). Figure 9 shows estimated isotopic signals of vegetation,
431	calculated from carbon isotope values of bone apatite of bats. Considering that fractionation
432	factors and isotope values in the mixing model are reasonably assumed (see Supplementary
433	Article S1), C4-feeding insects explains more than 10 % of the total diet in six out of the eight
434	individuals analyzed in this study even with a large isotopic spacing between predatory insects
435	and plants (open circle in Figure 9). On average, the estimated $\delta^{13}C$ value of bulk plants is
436	25.4‰ (open circle), which is translated to 22% of C ₄ plants in the simple mixing model. On
437	Minami-Daito Island, C ₄ plants were introduced only by humans via sugarcane plantations.
438	Therefore, the unmistakable isotopic signal of C ₄ plants demonstrates that these individuals
439	coexisted with humans after 1900.
440	
441	
442	Group size and estimated ages of cave-dwelling bats on the Daito Islands



Two locally extinct bat species, *Miniopterus* sp. and *Rhinolophus* sp., once existed in the lifted atoll remotely located from the closest landmass. Based on the number of skeletal remains, Cave A was utilized by more individuals of *Miniopterus* sp. than *Rhinolophus* sp. Considering the taphonomic conditions of the Minami-Daito bats (unpermineralized, exposed on cave floor without any depositional cover, fast crystal growth around bones in tropical wet caves), we interpret that these skeletons are only a few thousand years old at most but probably even younger and that the two species occurred contemporarily in the paleontological sense.

FTIR spectra and SEM images suggest that the guano-like deposits on Minami-Daito

FTIR spectra and SEM images suggest that the guano-like deposits on Minami-Daito Island are most reasonably humic substances, which are the final constituent of the physicochemical degradation and microbial decomposition of organic matter, particularly plant materials (Stevenson, 1994). The hydroxyapatite crust under the bat skeleton was possibly formed from the interaction between bat guano and limestone/dolomite. Nevertheless, we deny the presence of large amounts of guano deposits in the caves, which suggests the skeletal remains are not resultant from large populations or those which utilized these caves for generations after generations.

Our humic samples from both Hoshino Cave and Cave A yielded similar ages of 4565 calBP (on the 3-point average) and 4640 calBP, respectively (Table S2), which we think provide the maximum age constraint for the bat species as the bat bones collected in this study were scattered nearby pellet-like humic particles in Cave A. A better age constraint was provided by stable carbon isotopes of the selected bat bones from Cave A. Isotopic signals of C₄ grass-feeding insects detected in various degrees from six out of eight individuals strongly indicate that some of the sampled bats lived after 1900.



In summary, small groups of bats might have been strayed to Minami-Daito Island by a recent sporadic event(s) such as a typhoon, and they did not survive on the island long probably due to strong anthropogenic stresses on the islands.

468

465

466

467

469

470

471

472

473

474

475

476

477

478

479

480

481

482

483

484

485

486

487

488

Extirpation of two cave-dwelling bat species on the Daito Islands

Our multiproxy approach to constrain the estimated ages of the Minami-Daito cavedwelling bats include hearing surveys of local residents on the Daito Islands. This survey was conducted by Dr. Hidetoshi Ohta on August 22 and October 28 in 1991 for a different purpose but happened to provide an imperfect yet interesting perspective regarding the extirpation of the bats (pers. comm. with H. Ohta on December 31, 2018 by YK and DF). According to his field notes, three men (Mr. Akamine, Mr. Nakama, Mr. Sunagawa; all in their 80s) commented that they witnessed "bats smaller than the Daito flying fox" in a cave during the daytime within a few years after the end of WWII. In the second survey, three other men (Mr. Toma, Mr. Suzuki, and Mr. Okiyama; two in their 80s, one in his 90s) commented that they also saw "baby flying foxes" in caves near "Hagu (rim)" before WWII. For local residents, the Daito flying fox is a typical mammal on the island. Thus, these bats are reasonably considered as *Miniopterus* sp. and/or Rhinolophus sp., as the Daito flying fox roosts in the canopies of trees during the daytime, not utilizing caves. If our interpretation is correct, a remnant population of these bats persisted until sometime after WWII, and the very last survivors could have been present until the 1950s, which is consistent with our taphonomic interpretation of the bones.

On Minami-Daito Island, the irreversible rapid change from tropical/subtropical forests to sugarcane fields was extraordinary following the arrival of early settlers/residents in 1899-1900 with heavy development by the 1930s. In addition to reducing favorable habitats for cave-



dwelling bats by opening the land and filling in sinkholes, there would have been other mortality causes. Many caves were used as natural storage and air-raid shelters during WWII. Cave A was a base of the Imperial Japanese Army during WWII. There are metal scraps, glass bottles, and wood plausibly derived from that age. Surface water also transports waste into caves. We found coal-like carbon particles in the guano-like samples while handpicking in the lab, which may be related to wasted carbon derived from old steam locomotives that existed from 1917 to 1983 to transport harvested sugarcane stalks as the railway track was run near Cave A (Kada, 2009). Chemical pesticides were introduced in sugarcane plantations, and the aerial spray of pesticides was conducted at least in the early 1970s (Editorial Committee of the History of Minami-Daito Village, 1990: p.1167). Considering the extremely rapid civilization on the small island, anthropogenic activities are undeniably responsible for the local extinctions of the last population of the cave-dwelling bat species.

Conservation paleobiology on tropical oceanic islands

Using a multidisciplinary approach, we were able to bracket the estimated chronological age of the Minami-Daito cave-dwelling bats, ranging from a maximum constrained age of 4,640 calBP (radiocarbon age of humin closely scattered with the bat bones in Cave A) to the 1950s (hearing survey record). Stable carbon isotopes of bone apatite provided unmistakable direct evidence that they existed after 1900 and reinforced the hearing survey record.

Despite rapid civilization and deforestation on the island throughout the 20th century, the Daito flying fox has been able to survive on the island. The Daito flying fox, which is designated as a critically endangered species (IA) in the National Red Data List of the Ministry of the Environment, Japan (RDB, 2020) and is thus of high concern for species conservation (Vincenot



et al., 2017), consumes fruits and flectal of flative species such as Chinese banyan (Ficus
microcarpa), Fiscus superba var. japonica, Ficus virgala, and fan palm trees (Livistoma
chinensis var. amanoi), but it also utilizes windbreak trees and street trees as a food source
(Kinjo, 2009). Flexible food preferences may explain how the Daito flying fox has survived
throughout anthropogenic damages as in the case of Pteropus dasymallus inopinatus on Okinawa
Island, which utilizes planted trees in urban areas as stable food sources (Nakamoto et al., 2007).
Regarding the presence of fossil bat species on an oceanic island, a similar case was
reported for an extinct endemic bat, Synemporion keana (lava-tube bat), from the Hawaiian
Islands, which are over 3800 km away from the nearest continental landmass (Ziegler et al.,
2016). Synemporion keana is a vespertilionid bat slightly smaller than the extant Hawaiian hoary
bat (Lasiurus cinereus semotus) that is known to have inhabited the Hawaiian Islands at least
until the earliest Polynesian cultural period because a fossil of S. keana was successfully
radiocarbon dated to 1670 BP (Ziegler et al., 2016). According to that study and the references
therein, those fossils were recovered from infilled deposits (soil, eolian deposit, pond deposit) or
exposed on the floor of limestone sinkholes, volcanic lava tubes, a piping cave, and a volcanic-
tuff cone crater. Similar to our studies, those fossils were not suitable for DNA extraction or
radiocarbon dating. They estimated a chronological range of the Hawaiian fossil bat species by
establishing the ¹⁴ C ages of both coexisting animal skeletons such as birds and rats and cultural
artifacts derived from the same stratigraphic level or nearby and the formation of volcanic caves
from which the fossils were found. Another interesting case of the late Holocene (<4,000 BP)
extirpation of bats is found on a tropical island in the Caribbean (Soto-Centeno and Steadman,
2015).



In this study, we revealed that two cave-dwelling bat species were extirpated from Minami-Daito Island without any zoological record when they existed. Minami-Daito Island used to be a home of three bat species, but only a single species survived from anthropogenic disturbance. Geological, geochemical, and paleontological approaches are useful to bracket chronological ranges of the two extirpated species. Chronological ranges of extirpated species should be estimated with higher accuracy to deduce causality of the local extinction events and subsequently to promote conservation of biodiversity on oceanic islands, which are generally vulnerable to anthropogenic factors.

Conclusions

Minami-Daito Island is an oceanic island that has never been connected to another landmass since its emergence. A few skeletons of *Rhinolophus* sp. were found during the 1970s from Hoshino Cave, the only tourist cave on the island (Shimojana, 1978). In this study, we found not only an additional skeleton of *Rhinolophus* sp. from Hoshino Cave but also a skeleton of the same species and more of *Miniopterus* sp. from another private cave. Because these bones, which were exposed on the floor of the tropical dolomite caves, did not preserve collagen for radiocarbon dating, we used multidisciplinary proxies to provide time constraints for estimated ages of the bats. Differing from a previous study, we obtained limited witnesses of cave-dwelling bats from before/during WWII and concluded the "guano-like" deposits commonly previously identified were humic substances formed ca. 4640 calBP, which gives the maximum age constraint for the extirpated bats. Their populations were never large and quickly shrank due to rapid and heavy deforestation for sugarcane plantations on the island. They were extirpated from Minami-Daito Island without any zoological record when they existed. This study highlights that





anthropogenic activities increase the mortality of animal species newly strayed into insular environments. Further taxonomic studies and analyses of morphological variation could elucidate the possible biogeographic origins of the strayed populations.

Acknowledgments

We deeply appreciate Shin-Ichiro Kawada (National Museum of Nature and Science, Japan for permitting us to access zoological collections at NMNS and assisting with fieldwork and Benjamin T. Breeden III (University of Utah) for providing constructive comments and English proofreading for the early draft. We are thankful to Katsuji Yoshida (Cave Exploration Pro-Guide Team Ciao!), Takeshi Matsushita (Cave Exploration Pro-Guide Team Ciao!), and Yukari Yamaguchi (Cave Exploration Pro-Guide Team Ciao!) for making a route map of Cave A and to Ken Ōyabu and Masaharu Hayakawa (Uekusa Gakuen University & Junior College) for permitting access to modern bat guano in Taito, Isumi, Chiba. We are grateful to Yushi Osawa, Keiko Osawa, Yu Iijima, and Hiroko Nagaoka for field assistance and to Mika Yagishita and Sonoko Suzuki for lab assistance. Nozomi Suzuki provided us great support for isotope analyses.

Journal editors and reviewers are granted to be acknowledged.

Y.K. was financially supported by the Fujiwara Natural History Foundation (2018), the National Museum of Nature and Science as part of a research project called "Chemical Stratigraphy and Dating as a Clue for Understanding the History of the Earth and Life", and the Generalitat de Catalunya (CERCA Programme). D.F. was financially supported by the 26th PRO NATURA FUND, Asahi Glass Foundation, and JSPS KAKENHI Grant Number 20H01979.



582 **Figure Captions** 583 584 Figure 1. Map of Minami-Daito Island, route map of a privately-owned Cave A, cave map of 585 Hoshino Cave. (A) Satellite map (Google Earth, 2020); (B) Map of Ryukyu Islands; (C) 586 Entrance of Cave A; (D) Route map of Cave A; (E) Map of Hoshino Cave (Simplified from a 587 map of Ehime University Expedition Club, 1972). Solid circles indicate sampling localities of 588 guano-like deposits, and open stars indicate sampling localities of cave-dwelling bat bones. 589 Figure 2. Various conditions of skeletal remains of *Miniopterus* sp. (A) partially articulated, not 590 covered by flowstone; (B) complete skull with fragmentary bones, not covered by flowstone; (C) 591 partially articulated, covered by flowstone on the cave floor; (D) almost fully articulated, 592 covered by flowstone (NMNS-PV 23770). 593 **Figure 3.** Skeletal remains of *Miniopterus* sp. on the slopes of stalagmite in Cave A. (A) Heavily 594 covered by stalagmite; (B) More heavily covered by stalagmite, whose locality is shown in Fig. 595 1D. 596 **Figure 4.** Optic and SEM images of guano references and guano-like deposit in Hoshino Cave. 597 (A-C) Guano-like deposit (H180120g5) collected from Hoshino Cave, Minami-Daito Island; (D, 598 E) Modern guano (R2) collected in Taito, China; (F, G) Fossil guano (R3) collected in Fujido 599 Cave, Gunma. 600 Figure 5. SEM and optical images of guano-like deposit in Cave A. (A, C) Fecal pellet-like 601 sample (Y180119g2). (B, D) Hydroxyapatite crust (Y160114g1), possibly derived from bat 602 feces. 603 Figure 6. FTIR spectra of guano references, guano-like deposits, and humic acid. (A) 604 Commercial fertilizer (R1); (B) Modern fecal pellet (R3); (C) Fossil guano (R4); (D, E) Guano-605 like deposits sampled in Cave A; (F, G) Guano-like deposits sampled in Hoshino Cave; (H) 606 humic acid (Dick et al., 2003); (I) humic acid extracted from municipal solid waste (Palumbo et 607 al., 2018). The numbers of Minami-Daito samples (4: Y180119g3, 5: Y180120g1, 6: 608 H180120g5) correspond to sampling localities in Figs. 1D-1E. u: upper, b: bottom.



609	Figure 7. FTIR spectra of lateric soil, fissure-filled deposit, sampled deposits, and
610	hydroxyapatite. (A) Whole soil of Latosol (Dick et al., 2003); (B) Fissure-filled deposit; (C)
611	Guano-like deposit; (D) Hydroxyapatite crust; (E) Hydroxyapatite (Jayaweera et al., 2008). The
612	numbers of Minami-Daito samples (1: Fissure-filled deposit, 2: Y160114g1, 3: Y180119g2)
613	correspond to sampling localities in Fig. 1D.
614	Figure 8. Isotopic composition of carbon and nitrogen, total nitrogen by weight percent (%N),
615	and C:N ratio in selected guano-like samples and guano references, corresponding to Table 2.
616	(A) Stable nitrogen isotope values vs. %N; (B) Stable carbon isotope values vs. C:N. u: upper,
617	m: middle, b: bottom. Raw data are provided in Table S1. A full description of the bat guano
618	references (R1-R4) is in Supplementary Article S1.
619	Figure 9. Estimated δ^{13} C values of vegetation on Minami-Daito Island, calculated from bone
620	apatite $\delta^{13}C$ values of the cave-dwelling bats. Measured $\delta^{13}C$ values of bone apatite are provided
621	in Table 3. For the isotopic enrichment factors and $\delta^{13}C$ values of pure C_3 - and C_4 -vegetation
622	applied in this study, see Supplementary Article S1 for details.
623	
624	Table Captions
625	
626	Table 1. A list of skeletal remains of <i>Miniopterus</i> sp. and <i>Rhinolophus</i> sp. collected from
627	Minami-Daito Island, Okinawa. At the National Museum of Nature and Science (Tokyo, Japan),
628	all vertebrate fossils cataloged in the Department of Geology and Paleontology start with the
629	prefix "NMNS-PV".
630	
631	Table 2. Summary of carbon and nitrogen isotopes, C:N ratios, weight percent of carbon and
632	nitrogen in guano-like samples.
633	
634	Table 3. Stable carbon isotope values of bone apatite in the Minami-Daito cave-dwelling bats.



635	
636	Supplementary Information
637	Table S1. Isotopic composition of carbon and nitrogen, total nitrogen by weight percent (%N),
638	and C:N ratio in selected guano-like samples and guano references, corresponding to Table 2 and
639	Fig. 8.
540	Table S2. Summary of radiocarbon ages (calBP) of a fossil guano reference and Minami-Daito
641	samples.
542	
543	
544	Author Contributions
545	Yuri Kimura conceived and designed the experiments, performed the experiments, analyzed the
646	data, prepared figures and/or tables, authored or reviewed drafts of the paper, and approved the
547	final draft.
548	
549	Other authors reviewed drafts of the paper and approved the final draft
650	
651	
552	
653	
654	
655	References
656	
657	Bronk Ramsey C. 2009. Bayesian analysis of radiocarbon dates. <i>Radiocarbon</i> 51(1): 337–360.
658	DOI 10.1017/S0033822200033865.
659 660 661	Cerling TE, Harris JM, MacFadden BJ, Leakey MG, Quade J, Eisenmann V, Ehleringer JR. 1997. Global vegetation change through the Miocene/Pliocene boundary. <i>Nature</i> 389: 153–158. DOI 10.1038/38229.

002

663	Chen SF, Juan C, Rossite S, Kinjo T, Fukui D, Kawai K, Tsang SM, Veluz MJ, Sakurai H, Jang-
664	Liaw NH, Osawa K, Ko WY, Izawa M. 2021. Population genetic structure of the insular
665	Ryukyu flying fox Pteropus dasymallus. Biotropica 3: 979211. DOI 10.1111/btp.12897.
666	Dick DP, Santos JHZ, Ferranti EM. 2003. Chemical Characterization and Infrared Spectroscopy
667	of Soil Organic Matter from Two Southern Brazilian Soils. Revista Brasileira de Ciência do
668	Solo 27(1): 29–39. DOI 10.1590/s0100-06832003000100004.
669	Editorial Committee of the History of Minami-daito Village. 1990. [The History of Minami-daito
670	Village]. A revised edition. Minami-daito Village Office, Naha [in Japanese]
671	Ehime University Expedition Club. 1972. [Caves on Minami-Daito Island]. Report on the 8th
672	Exploration of the Ryukyu Islands. [in Japanese]
673	Fiore S, Laviano R. 1991. Brushite, hydroxylapatite, and taranakite from Apulian caves
674	(southern Italy): New mineralogical data. <i>American Mineralogist</i> 76(9–10): 1722–1727.
675	Forbes MS., Bestland, EA. 2006. Guano-derived deposits within the sandy cave fills of
676	Naracoorte, South Australia. Alcheringa: An Australasian Journal of Palaeontology 1: 129-
677	146. DOI 10.1080/03115510609506859.
678	Giurgiu A, Tămaş, T. 2013. Mineralogical data on bat guano deposits from three Romanian
679	caves. Studia Universitatis Babes-Bolyai, Geologia 58(2): 13-18. DOI 10.5038/1937-
680	8602.58.2.2.



681	Google Earth V7.3.3.7786 (July 21, 2020) Minami-Daito, Okinawa, Japan. 25 50'27.86"N, 131
682	14'35.24"E, Eye alt 11.81km. Landsat/Copernicus, Maxar Technologies 2021, CNES/Airbus
683	2012. http://www.earth.google.com [accessed May 17, 2021].
684	Gratton C, Forbes AE. 2006. Changes in δ^{13} C stable isotopes in multiple tissues of insect
685	predators fed isotopically distinct prey. <i>Oecologia</i> 147(4): 615–624. DOI 10.1007/s00442-
686	005-0322-y.
687	Hill CA, Forti P. 1997. Cave Minerals of the World, second edition. Huntsville, Alabama:
688	National Speleological Society, 463 p.
689	Inskeep WP, Silvertooth JC. 1998. Inhibition of hydroxyapatite precipitation in the presence of
690	fulvic, humic, and tannic acids. Soil Science Society of America Journal 52: 941–946.
691	Jayaweera HDAC, Siriwardane I, de Silva KMN, de Silva RM. 2018. Synthesis of
692	multifunctional activated carbon nanocomposite comprising biocompatible flake nano
693	hydroxyapatite and natural turmeric extract for the removal of bacteria and lead ions from
694	aqueous solution. Chemistry Central Journal 12(1): 1-14. DOI 10.1186/s13065-018-0384-
695	7.
696	Kada Y. 2009. Remember sugarcane railway on Minami-Daito Island. In: [The People and
697	Nature of Minami Daito Island]. Ed. Seiichi Nakai, Kazuaki Higashi and Daniel Long,
698	104–120. Kagoshima: Nampo Shinsha. [in Japanese]
699	Kaya M, Seyyar O, Baran T, Turkes T. 2014. Bat guano as new and attractive chitin and chitosan
700	source. Frontiers in Zoology 11: 59. DOI 10.1186/s12983-014-0059-8.



01	Kinjo K. 2009. [Bats Living in a Remote Oceanic Island]. In: [The People and Nature of Minami
02	Daito Island]. Ed. Seiichi Nakai, Kazuaki Higashi and Daniel Long, 138-150. Kagoshima:
03	Nampo Shinsha. [in Japanese]
'04	Klein GV, Kobayashi K. 1980. Geological summary of the North Philippine Sea, based on Deep
'05	Sea Drilling Project Leg 58 Results. In Klein GV, Kobayashi K., eds. Initial Reports of the
'06	Deep Sea Drilling Project 58. U.S. Government Printing Office, 951–961. DOI
07	10.2973/dsdp.proc.58.144.1980.
'08	Kohn MJ 2010. Carbon isotope compositions of terrestrial C3 plants as indicators of
'09	(paleo)ecology and (paleo)climate. Proceedings of the National Academy of Sciences of the
10	United States of America 107(46): 19691–19695. DOI 10.1073/pnas.1004933107.
11	Méndez J. 1967. Organic compounds in humic acid extracts. <i>Geoderma</i> 1(1): 27–36. DOI
12	10.1016/0016-7061(67)90012-2.
13	Nakamoto A, Kinjo K, Izawa M. 2007. Food habits of Orii's flying-fox, <i>Pteropus dasymallus</i>
14	inopinatus, in relation to food availability in an urban area of Okinawa-jima Island, the
15	Ryukyu Archipelago, Japan. Acta Chiropterologica 9(1): 237–249. DOI 10.3161/1733-
16	5329(2007)9[237:FHOOFP]2.0.CO;2.
17	Nambu A, Inagaki S, Ozawa S, Suzuki Y, Iryu Y. 2003. Stratigraphy of reef deposits on Kita-
18	daito-jima, Japan. Journal of Geological Society of Japan 109(11): 617-634. [in Japanese
19	with English summary]



720	Ohde S., Elderfield H. 1992. Strontium isotope stratigraphy of Kita-daito-jima Atoll, North
721	Philippine Sea: implications for Neogene sea-level change and tectonic history. Earth and
722	Planetary Science Letters 113(4): 473–486. DOI 10.1016/0012-821X(92)90125-F.
723	Omori T, Yamazaki K, Itahashi Y, Ozaki H, Yoneda M. 2017. Development of a simple
724	automated graphitization system for radiocarbon dating at the University of Tokyo. 14th
725	International Conference on Accelerator Mass Spectrometry, University of Ottawa,
726	Canada.
727	Ota Y, Omura A, Koba M, Kawana T, Miyauchi T. 1991. Late Quaternary tectonic movements
728	as deduced from raised coral reefs of Daito Islands on the northwestern part of Philippine
729	Sea Plate. <i>Journal of Geography</i> 100(3): 317–336. [in Japanese with English summary]
730	Palumbo G, Schiavon M, Nardi S, Ertani A, Celano G, Colombo CM. 2018. Biostimulant
731	potential of humic acids extracted from an amendment obtained via combination of olive
732	mill wastewaters (OMW) and a pre-treated organic material derived from municipal solid
733	waste (MSW). Frontiers in Plant Science 9: 1028. DOI 10.3389/fpls.2018.01028.
734	Podlesak DW, Torregrossa A-M, Ehleringer JR, Dearing MD, Passey BH, Cerling TE. 2008.
735	Turnover of oxygen and hydrogen isotopes in the body water, CO ₂ , hair, and enamel of a
736	small mammal. Geochimica et Cosmochimica Acta 72: 19–35. DOI
737	10.1016/j.gca.2007.10.003.
738	RDB, 2020. [Japanese Red Data Book]. Japan Integrated Biodiversity Information System.



/39	Reimer P, Austin WEN, Bard E, Bayliss A, Blackwell PG, Bronk Ramsey C, Butzin M, Cheng
740	H, Lawrence Edwards R, Friedrich M, Grootes PM, Guilderson TP, Hajdas I, Heaton TJ,
741	Hogg AG, Hughen KA, Kromer B, Manning SW, Muscheler R, Talamo, S. (2020). The
742	IntCal20 Northern Hemisphere radiocarbon age calibration curve (0-55 cal kBP).
743	Radiocarbon 62(4): 725-757. DOI 10.1017/RDC.2020.41.
744	Salvarina I, Yohannes E, Siemers BM, Koselj K. 2013. Advantages of using fecal samples for
745	stable isotope analysis in bats: Evidence from a triple isotopic experiment. Rapid
746	Communications in Mass Spectrometry 27(17): 1945–1953. DOI 10.1002/rcm.6649.
747	Schmidt MWI, Gleixner G. 2005. Carbon and nitrogen isotope composition of bulk soils,
748	particle-size fractions and organic material after treatment with hydrofluoric acid. European
749	Journal of Soil Science 56(3): 407–416. DOI 10.1111/j.1365-2389.2004.00673.x.
750	Seno T, Maruyama S. 1984. Paleogeographic reconstruction and origin of the Philippine Sea.
751	Tectonophysics 102: 53–84. DOI 10.1016/0040-1951(84)90008-8.
752	Shimojana M. 1978. [Cave faunas on Minami- and Kita-daito-jima Islands and the southern part
753	of Okinawa-jima Island]. In: Board of Education, Okinawa Prefecture, ed. [Survey Report
754	on Caves in Okinawa Prefecture I]. Board of Education, Okinawa Prefecture, Naha, 75-
755	111. [in Japanese]
756	Soto-Centeno JA, Steadman, DW. 2015. Fossils reject climate change as the cause of extinction
757	of Caribbean bats. Scientific Reports 5: 7971. DOI 10.1038/srep07971.



758	Stevenson FJ. 1994. Humus Chemistry: Genesis, Composition, Reactions (2nd ed.). New York:
759	John Wiley & Sons.
760	Stuiver M, Polach HA. 1977. Discussion reporting of ¹⁴ C data. <i>Radiocarbon</i> 19(3): 355–363.
761	Tămaș T, Miheț O, Giurgiu A. 2014. Mineralogy of bat guano deposits from Huda lui papară
762	cave (Trascău Mountains, Romania). Carpathian Journal of Earth and Environmental
763	Sciences 9(3): 25–32.
764	Urushibara-Yoshino K. 2012. Karstification processes on Minamidaito Island in the Nansei
765	Archipelago, southwest Japan. Bulletin of the Faculty of Letters, Hosei University 65: 83-
766	95. [in Japanese with English summary]
767	van der Geer A, Lyras G, de Vos J, Dermitzakis D. 2010. Evolution of Island Mammals:
768	Adaptation and Extinction of Placental Mammals on Islands. Oxford: Wiley-Blackwell.
769	DOI 10.1002/9781444323986.
770	Vincenot CE, Collazo AM, Russo D. 2017. The Ryukyu flying fox (<i>Pteropus dasymallus</i>)—A
771	review of conservation threats and call for reassessment. <i>Mammalian Biology</i> 83: 71–77.
772	DOI 10.1016/j.mambio.2016.11.006.
773	Wurster CM, Bird MI, Bull ID, Creed F, Bryant C, Dungait JAJ, Paz V. 2010. Forest contraction
774	in north equatorial Southeast Asia during the Last Glacial Period. Proceedings of the
775	National Academy of Sciences 107(35): 15508–15511. DOI 10.1073/pnas.1005507107.
776	Zhang W, Jiang S, Wang K, Wang L, Xu Y, Wu Z, Shao H, Wang Y, Miao M. 2015.
777	Thermogravimetric dynamics and FTIR analysis on oxidation properties of low-rank coal at



PeerJ

778	low and moderate temperatures. International Journal of Coal Preparation and Utilization
779	35(1): 39–50. DOI 10.1080/19392699.2013.873421.
780	Ziegler AC, Howarth FG, Simmons NB. 2016. A second endemic land mammal for the
781	Hawaiian Islands: a new genus and species of fossil bat (Chiroptera: Vespertilionidae).
782	American Museum Novitates 3854: 1–52.
783	
784	
785	
786	
787	
788	
789	



Figure 1. Map of Minami-Daito Island, route map of a privately-owned Cave A, cave map of Hoshino Cave.

(A) Satellite map (Google Earth, 2020); (B) Map of Ryukyu Islands; (C) Entrance of Cave A; (D) Route map of Cave A; (E) Map of Hoshino Cave (Simplified from a map of Ehime University Expedition Club, 1972). Solid circles indicate sampling localities of guano-like deposits, and open stars indicate sampling localities of cave-dwelling bat bones.



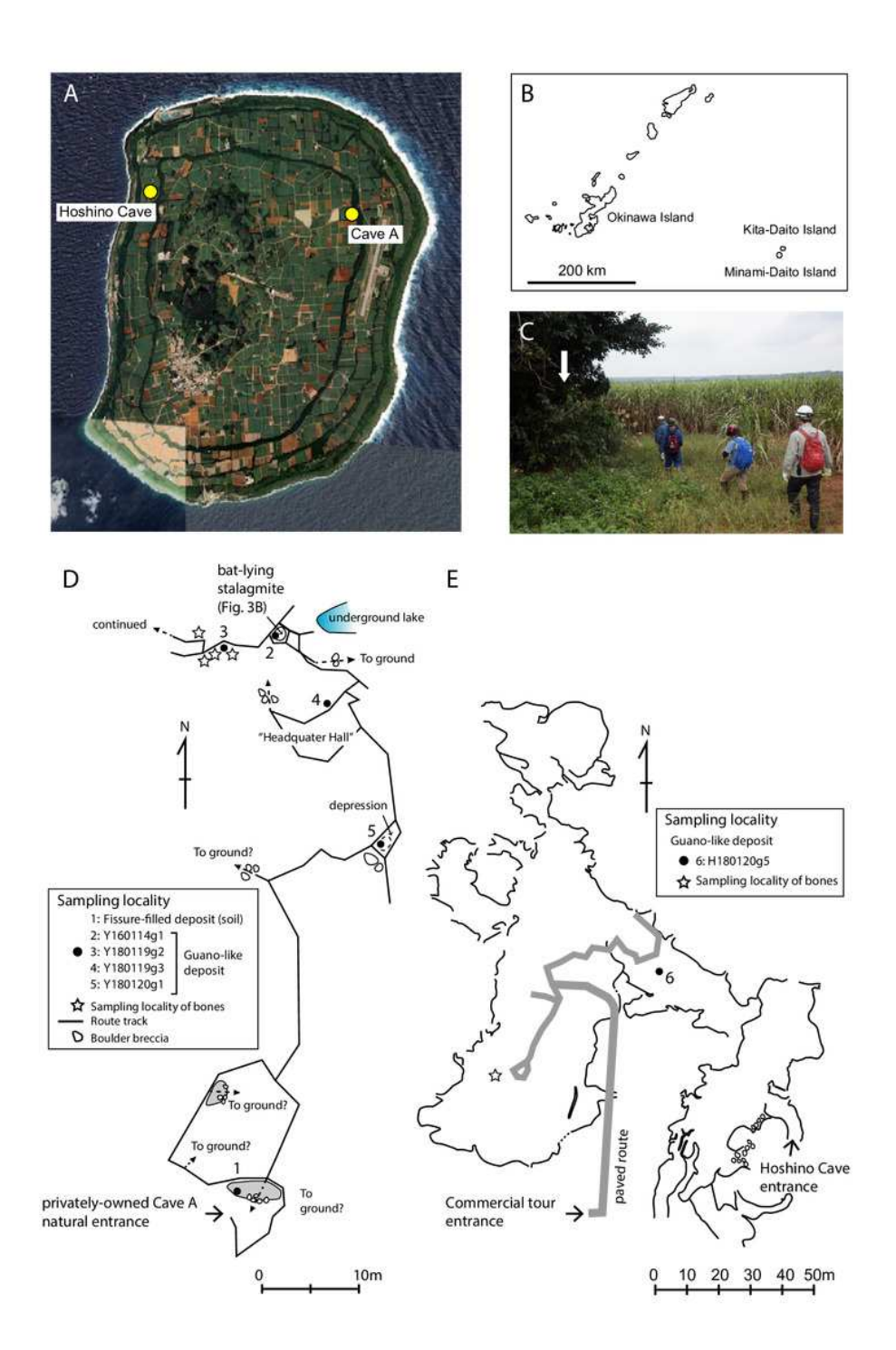




Figure 2. Various conditions of skeletal remains of *Miniopterus* sp.

(A) partially articulated, not covered by flowstone; (B) complete skull with fragmentary bones, not covered by flowstone; (C) partially articulated, covered by flowstone on the cave floor; (D) almost fully articulated, covered by flowstone (NMNS-PV 23770).



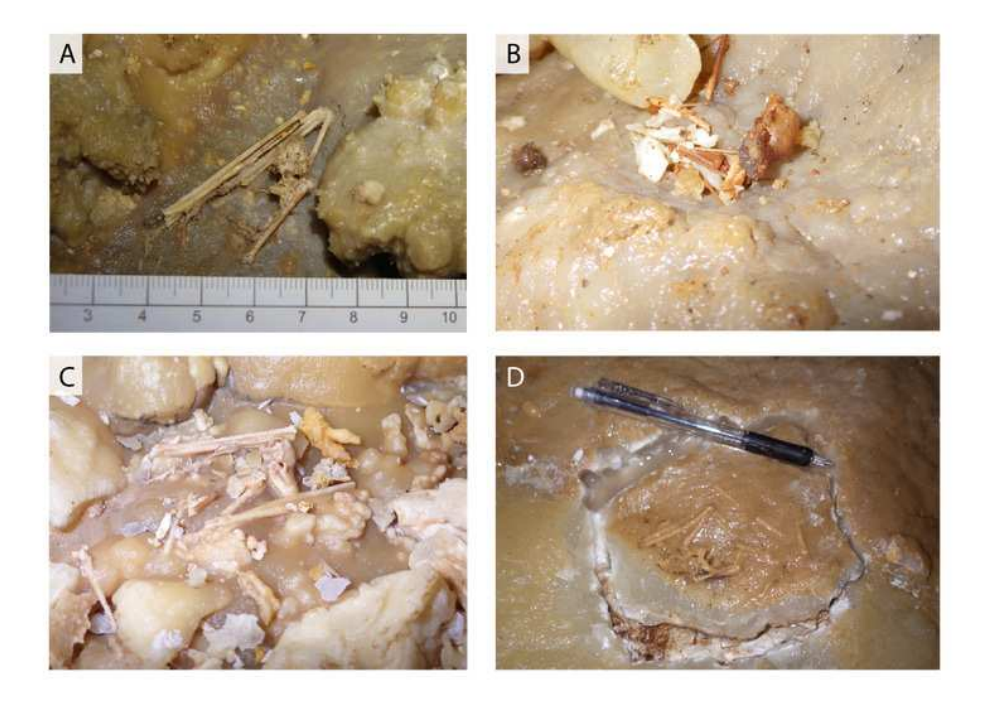
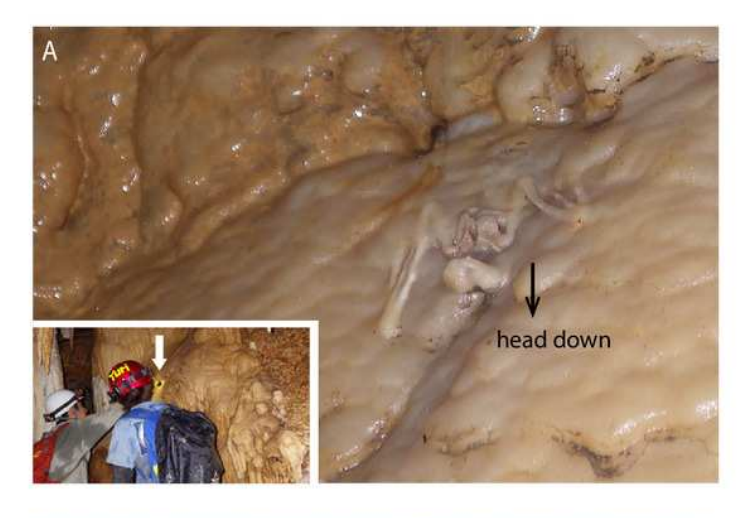




Figure 3. Skeletal remains of *Miniopterus* sp. on the slopes of stalagmite in Cave A.

(A) Heavily covered by stalagmite; (B) More heavily covered by stalagmite, whose locality is shown in Fig. 1D.





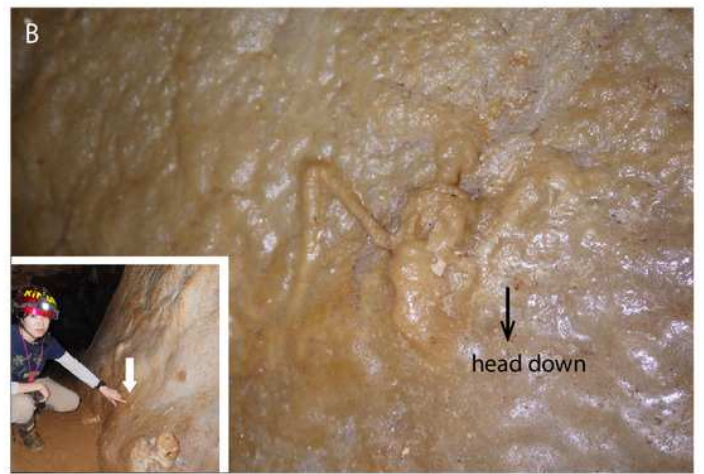




Figure 4. Optic and SEM images of guano references and guano-like deposit in Hoshino Cave.

(A-C) Guano-like deposit (H180120g5) collected from Hoshino Cave, Minami-Daito Island; (D,

E) Modern guano (R2) collected in Taito, China; (F, G) Fossil guano (R3) collected in Fujido Cave, Gunma.

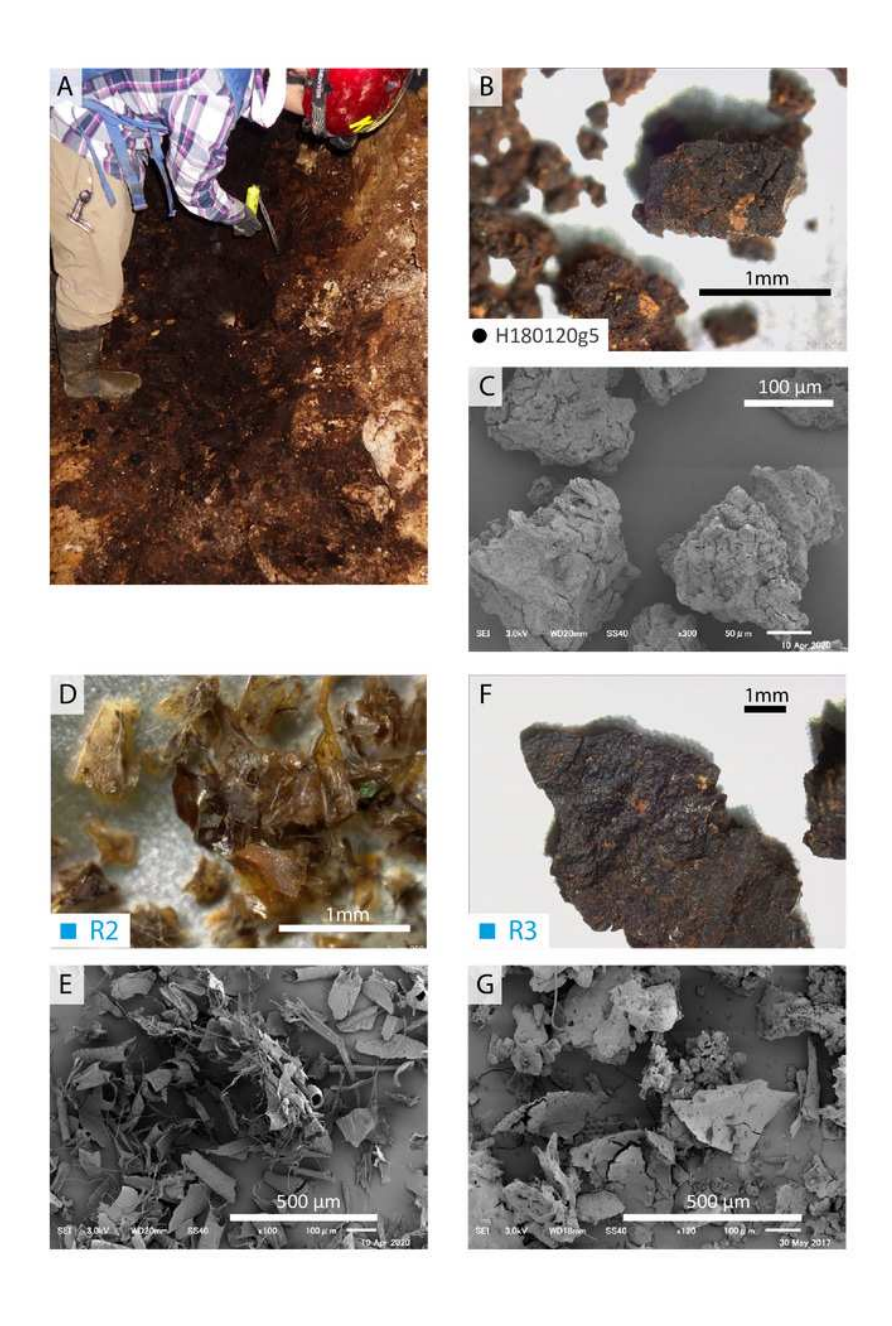




Figure 5. SEM and optical images of guano-like deposit in Cave A.

(A, C) Fecal pellet-like sample (Y180119g2). (B, D) Hydroxyapatite crust (Y160114g1), possibly derived from bat feces.



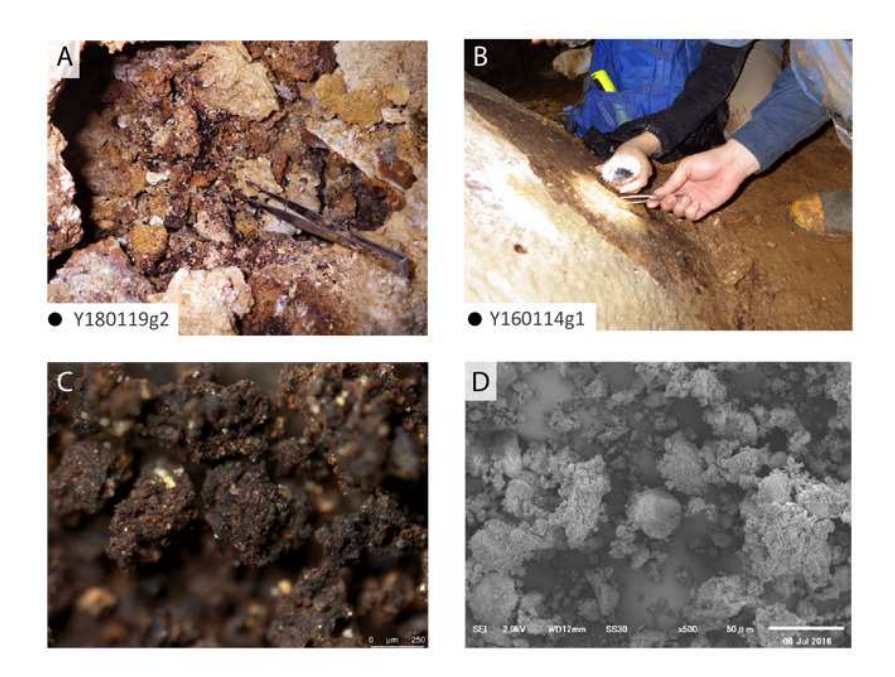




Figure 6. FTIR spectra of guano references, guano-like deposits, and humic acid.

(A) Commercial fertilizer (R1); (B) Modern fecal pellet (R3); (C) Fossil guano (R4); (D, E) Guano-like deposits sampled in Cave A; (F, G) Guano-like deposits sampled in Hoshino Cave; (H) humic acid (Dick et al., 2003); (I) humic acid extracted from municipal solid waste (Palumbo et al., 2018). The numbers of Minami-Daito samples (4: Y180119g3, 5: Y180120g1, 6: H180120g5) correspond to sampling localities in Figs. 1D-1E. u: upper, b: bottom.



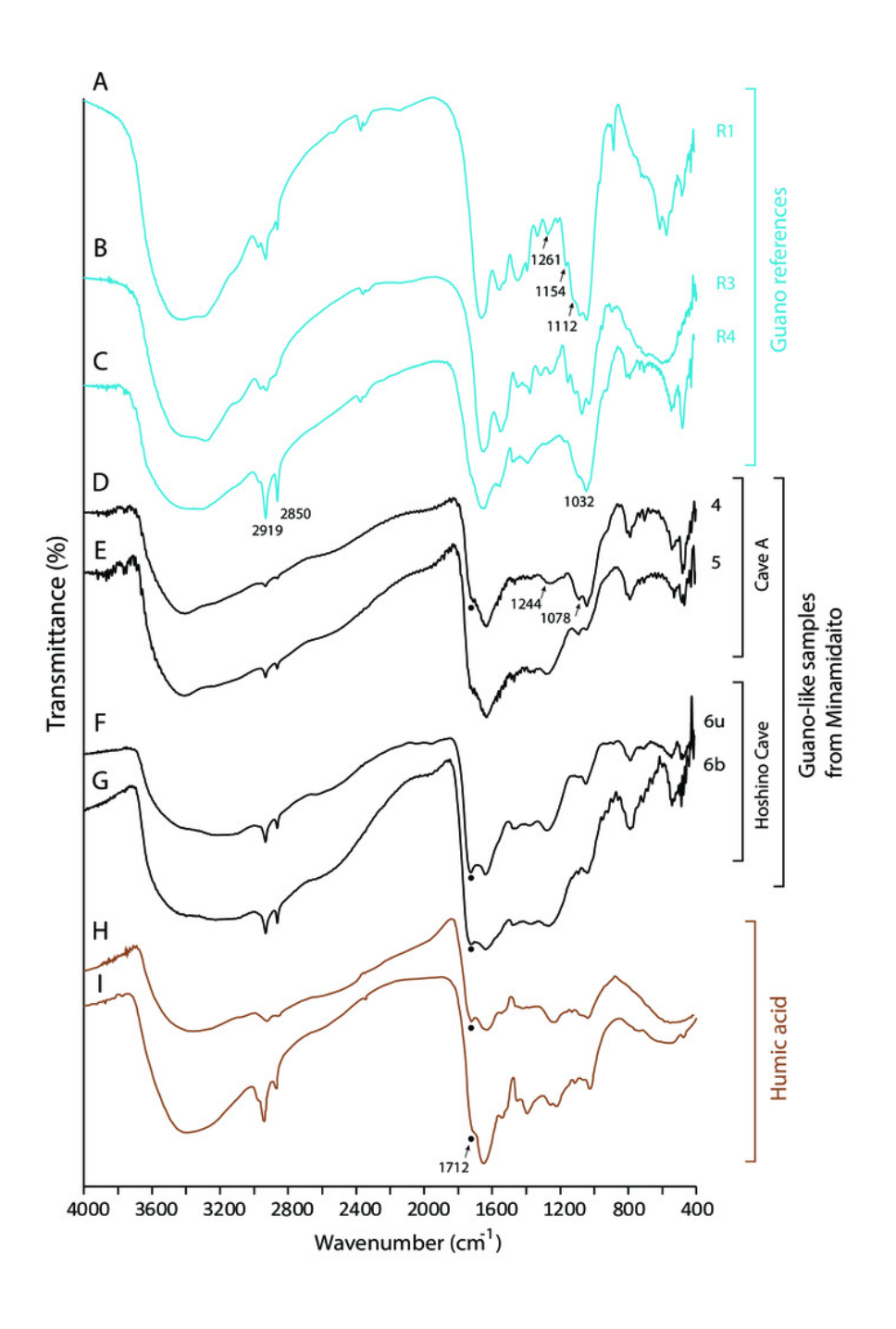




Figure 7. FTIR spectra of lateric soil, fissure-filled deposit, sampled deposits, and hydroxyapatite.

- (A) Whole soil of Latosol (Dick et al., 2003); (B) Fissure-filled deposit; (C) Guano-like deposit;
- (D) Hydroxyapatite crust; (E) Hydroxyapatite (Jayaweera et al., 2008). The numbers of Minami-Daito samples (1: Fissure-filled deposit, 2: Y160114g1, 3: Y180119g2) correspond to sampling localities in Fig. 1D.



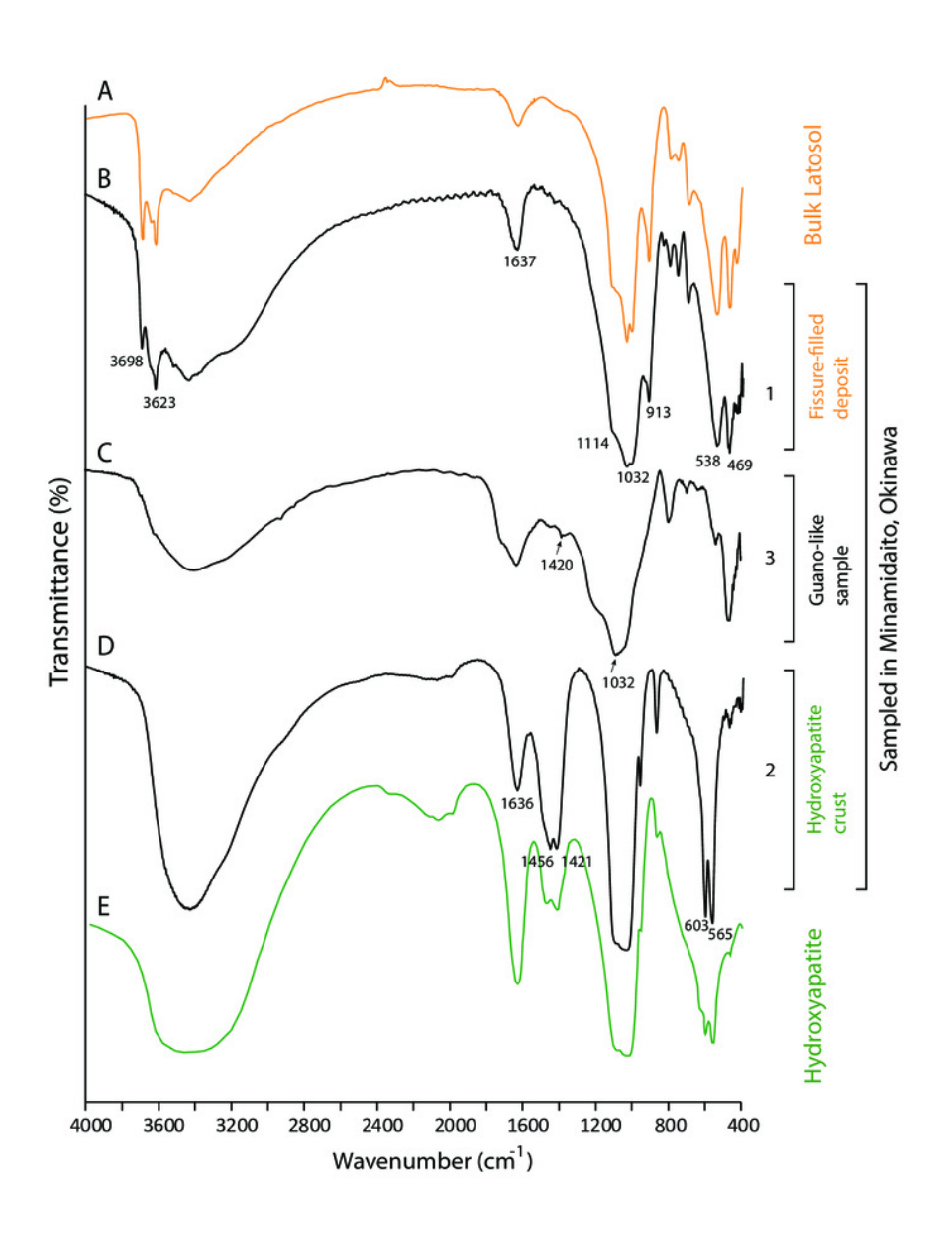
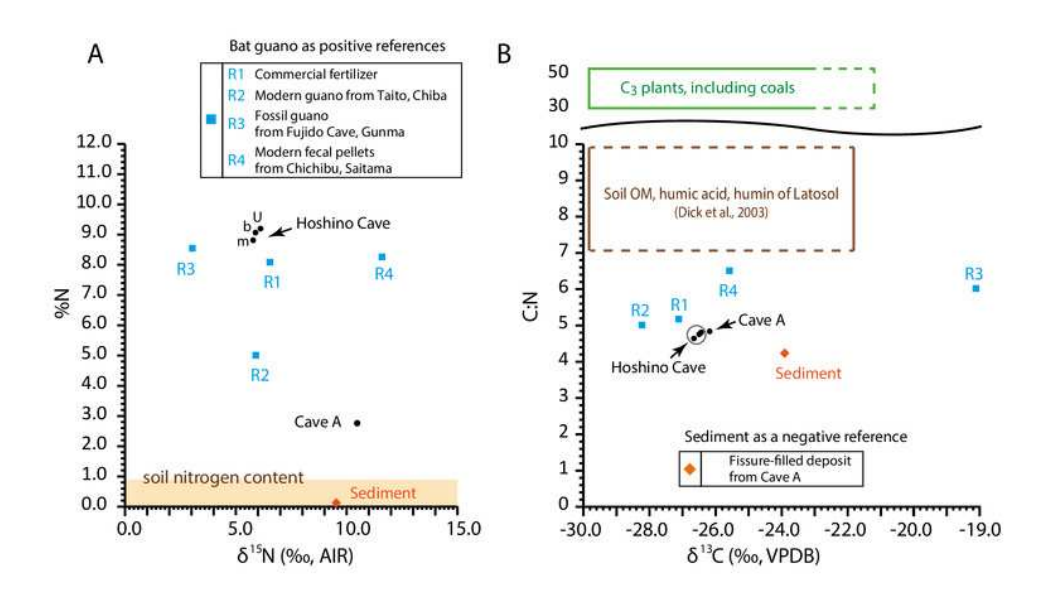




Figure 8. Isotopic composition of carbon and nitrogen, total nitrogen by weight percent (%N), and C:N ratio in selected guano-like samples and guano references, corresponding to Table 2.

(A) Stable nitrogen isotope values vs. %N; (B) Stable carbon isotope values vs. C:N. u: upper, m: middle, b: bottom. Raw data are provided in Table S1.







Estimated $\delta^{13}C$ values of vegetation on Minami-Daito Island, calculated from bone apatite $\delta^{13}C$ values of the cave-dwelling bats.

Measured δ^{13} C values of bone apatite are provided in Table 3. For the isotopic enrichment factors and δ^{13} C values of pure C_3 - and C_4 -vegetation applied in this study, see Supplementary Article S1 for details.



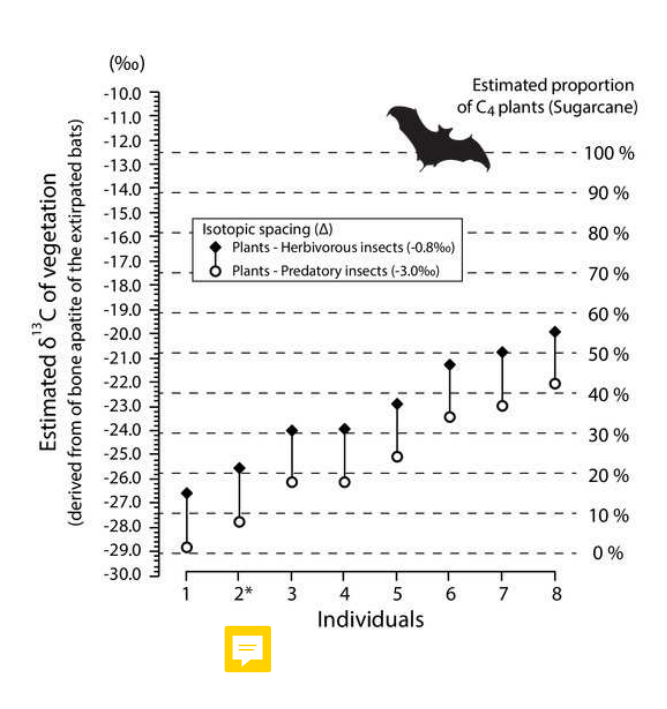




Table 1(on next page)

Table 1. A list of skeletal remains of *Miniopterus* sp. and *Rhinolophus* sp. collected from Minami-Daito Island, Okinawa.

At the National Museum of Nature and Science (Tokyo, Japan), all vertebrate fossils catalogued in the Department of Geology and Paleontology start with the prefix "NMNS-PV".

PeerJ

Table 1

Table 1						
Museum ID (NMNS-PV)	NMNS-PV branch number	Scientific name	Estimated # of individual	Identification	Cave	Field Sampling ID
23770		Miniopterus sp.	1	Articulated body	Cave A	NA
23771		Miniopterus sp.	1	Articulated body	Cave A	NA
	1			Left maxilla with two molars (partial)		H160114-01-G
	2			Left mandible with teeth (m1-m3)		H160114-01-A
	3			Right mandible without teeth (partial, fragmented)		H160114-01-F
	4	1		Left radius (partial)		H160114-01-C
23772	5	- Rhinolophus sp.	1	Radius? (partial)	Hoshino Cave	H160114-01-E
	6, 7			Pelvic bone (fragment), rib (partial),		H160114-01-B
	8			Left humerus (almost complete)		H160114-01-D
	NA			Skull (zygomatic arch only), bone fragments		H160114-01-H
	1			Left maxilla with teeth (partial)		Y160113-10-C
	2			Left mandible (fragment)		Y160113-10-G
	3,4,5,6,7,8,9			Right mandible with teeth (fragmented)		Y160113-10-B
	10			Left clavicle (complete)		Y160113-10-D
	11			Left radius (fragment)		Y160113-10-H
23773	12	Rhinolophus sp.	1	Radius? (fragment, small rod branched off), bone fragments	Cave A	Y160113-10-J
	13	-		Left humerus (partial)		Y160113-10-I
	14			Pelvic bone (almost complete), bone fragment		Y160113-10-A
	15	1		Metacarpal or phalange (partial)?		Y160113-10-E
	16	1		Metacarpal? (partial)		Y160113-10-K
	NA	1		Bone fragment (could not identified by YK)		Y160113-10-F

	NA			Bone fragments		Y160113-10-L
	1			Left radius (fragment)		Y160113-04-B
	2			Right radius (complete)		Y160113-04-D
	3			Left humerus (fragment)		Y160113-04-E
23774	4	Miniopterus sp.	1	Right humerus (complete)	Cave A	Y160113-04-C
	5			Metacarpal (fragment)		Y160113-04-J
	6,7			Metacarpal or phalange? (fragments)		Y160113-04-A
	NA			Bone fragments		Y160113-04-G
23775		Miniopterus sp.	1	Right radius (complete)	Cave A	Y160113-05-A
23776		Miniopterus sp.	1	Right radius (almost complete)	Cave A	Y160113-06-A
	1			Skull		Y160113-08-F
	2		1	Left radius (partial)		Y160113-08-A
23777	3	Miniopterus sp.		Left humerus (complete)	Cave A	Y160113-08-E
23///	4			Right humerus (fragment)	Cave A	Y160113-08-D
	5			Metacarpal (fragment)		Y160113-08-G
	NA			Bone fragments		Y160113-08-B
	1			Skull (partial, fragment) without teeth		Y160113-03-A
	2,3,4,5,6,7,8			Isolated teeth		Y160113-03-B
	9			Right dentary wo teeth		Y160113-03-K
23778	10,11,12,13,14,15,16,18,19,20,21	<i>Miniopterus</i> sp.	1	Left dentary, five islated teeth	Cave A	Y160113-03-I
	22			Isolated tympanic bulla (partial)	1	Y160113-03-O
	23,24			Scapula (fragment), skull (zygomatic arch only)		Y160113-03-N
	25			Right radius (fragment)		Y160113-03-C

	26			Right humerus		Y160113-03-H
	27,28,29			Metacarpal		Y160113-03-E
	30			Metacarpal, metacarpal or phalange? (fragments)		Y160113-03-F
	31			Metacarpal (fragment)		Y160113-03-J
	32			Metacarpal or phalange? (fragment)		Y160113-03-M
	33,34,35,36			Rib		Y160113-03-D
	NA			Bone fragment (radius, left or right unidentified)		Y160113-03-G
	NA			Bone fragment (radius, left or right unidentified)		Y160113-03-L
	NA			Bone fragments		Y160113-03-P
	1			Skull (maxilla with ful dentition, others fragmented)		Y160114-01-A
	2		1	Right mandible with dentition (almost complete)		Y160114-01-G
	3			Isolated antemolar		Y160114-01-G
22770	4			Atlas (complete)		Y160114-01-E
23779	5	Miniopterus sp.		Left radius (fragment)	Cave A	Y160114-01-C
	6			Right radius (almost complete)		Y160114-01-F
	7			Left humerus (complete)		Y160114-01-B
	8			Right humerus (complete)		Y160114-01-D
	9			Left femur (complete)		Y160114-01-H
	NA			Bone fragments		Y160114-01-I
	1			Skull		Y160114-02-A
23780	2	Miniopterus sp.	1	Left mandible	Cave A	Y160114-02-D
23/00	3,4,5	Ινιιποριεί ας δρ.	1	Axis, cervical bones	Cave A	Y160114-02-F
	6			Thoracic vertebrate (partial)		Y160114-02-J

	7			Clavicle (complete)		Y160114-02-I
-	8			Left scapula (partial)	_	Y160114-02-G
-	9			Left radius (complete)	_	Y160114-02-H
	10			Left humerus (fused with other bones by calcite crystals)		Y160114-02-E
	11			Right humerus (partial)		Y160114-02-B
-	12,13			Metacarpals (partial)		Y160114-02-C
	14,15,16,17,18,19,20			Ribs		Y160114-02-K
	NA			Metacarpals or carpal (fragment)	_	Y160114-02-M
	NA			Bone fragment		Y160114-02-L
	1			Skull (partial), skull fragments		Y160114-03-A
	2,3,4,5,6,7			temparate bullae, isolated teeth		Y160114-03-I
	8			Left radius (complete)		Y160114-03-C
	9			Right radius (complete)		Y160114-03-B
	10			Left humerus (fragment)		Y160114-03-H
22704	11	Miniantana	1	Right humerus (complete)		Y160114-03-G
23781	12	<i>Miniopterus</i> sp.	1	Right femur	Cave A	Y160114-03-E
	13			Metacarpal (partial)		Y160114-03-D
	14			Metacarpal (partial)		Y160114-03-J
	15			Metacarpal (partial)		Y160114-03-K
	16			Metacarpal (partial)		Y160114-03-L
	NA			Metacarpal (fragment)		Y160114-03-F
	1			Left maxila with dentition (partial)		Y160114-04-E
23782	2,3	Miniopterus sp.	1	Left dentary with dentition (complete), isolated m1 (trigonid basin only)	Cave A	Y160114-04-C
	4,5			Right dentary with dentition (complete), isolated antemolar		Y160114-04-D

	6			Right radius (partial)		Y160114-04-B
	NA			Metacarpal or phalange (fragments)		Y160114-04-A
	NA			Bone fragments		Y160114-04-F
	1			Left radius (partial)		Y160113-07-B
	2			Left? radius (fragment)		Y160113-07-D
	3			Right radius (complete)		Y160113-07-E
	4			Right? radius (fragment)	Cave A	Y160113-07-K
23783	5	Miniopterus sp.	2	Left humerus (complete)		Y160113-07-F
	6			Left humerus (complete)		Y160113-07-A
	7			Right humerus (complete)		Y160113-07-G
	8			Right humerus, bone fragment		Y160113-07-C
	NA			Metacarpal or phalange? (bone fragments)		Y160113-07-H
23784		<i>Miniopterus</i> sp.	1	Left and right mandibles (complete, separated)	Cave A	
23785		Miniopterus sp.	1	Right maxilla with dentition (partial)	Cave A	
24999		Miniopterus sp.	1	Left mandible (partial)	Cave A	
25000		Miniopterus sp.	1	Right mandible (partial)	Cave A	



Table 2(on next page)

Table 2. Summary of carbon and nitrogen isotopes, C:N ratios, weight percent of carbon and nitrogen in samples.

1 Table 2 2

Sample ID	Material Type Sampling locality	N	δC (‰, VPDB)		δN (‰, AIR)		C/N		%C in sample		%N in sample		
Sample 15	Widterial Type	Sumpling locality	''	Average	SD	Average	SD	Average	SD	Average	SD	Average	SD
R1	Modern guano (R1)	Commercial fertilizer	5	-27.1	0.22	6.5	0.37	5.2	0.24	41.8	1.0	8.1	0.5
R2	Modern guano (R2)	Taito, Chiba	1	-28.2		5.9		5.0		44.8		8.9	
R3	Modern fecal pellet (R3)	Chichibu, Saitama	3	-19.1	0.03	3.0	0.10	6.0	0.02	51.1	0.4	8.6	0.1
R4	Fossil guano (R4)	Fujido Cave, Ueno, Gunma	1	-25.6		11.6		6.5		53.8		8.3	
Sediment	Fissure-filled cave deposit	#1 in Cave A	7	-23.9	0.15	9.5	0.17	4.2	0.24	0.5	0.03	0.1	0.002
Y180119g2	Fecal pellet-like sample	#3 in Cave A	1	-26.1		10.2		4.8		13.2		2.7	
H180120g5-u	Guano-like deposit	#6 in Hoshino Cave	1	-26.4		6.1		4.8		44.3		9.2	
H180120g5-m	Guano-like deposit	#6 in Hoshino Cave	1	-26.7		5.8		4.6	·	40.9		8.8	
H180120g5-b	Guano-like deposit	#6 in Hoshino Cave	1	-26.5		5.9		4.8	·	43.2		9.1	



Table 3(on next page)

Stable carbon isotope values of bone apatite in the Minami-Daito cave-dwelling bats.

1 Table 3

2

Individual #	Element	δ ¹³ C (‰, VPDB)	Lab Code
1	Proximal end of right humerus	-15.0	Y160113b-6
2	Multiple bone fragments	-14.0	Y160113b-201902-4-2
3	Distal end of right humerus	-12.4	Y160113b-8
4	Left radius	-12.3	Y160113b-201902-1
5	Right radius	-11.3	Y160113b-201902-2-2
6	Distal end of humerus	-9.6	Y160113b-5
7	Proximal end of femur	-9.1	Y160113b-7
8	Fragments of left humerus and left radius	-8.3	Y160113b-201902-3-2

3